More efficient AC filterless flexible LCC HVDC by analyzing the impact of single-phase fault on commutations

Yang, Conghuan; Xue, Ying; Zhang, Xiao-ping

DOI:
10.1109/ACCESS.2020.3048941

Document Version
Publisher's PDF, also known as Version of record

Citation for published version (Harvard):
Yang, C, Xue, Y & Zhang, X 2021, 'More efficient AC filterless flexible LCC HVDC by analyzing the impact of single-phase fault on commutations', *IEEE Access*, vol. 9, pp. 7643-7654.
https://doi.org/10.1109/ACCESS.2020.3048941

IEEE Access
Multidisciplinary | Rapid Review | Open Access Journal

Received December 20, 2020, accepted December 30, 2020, date of publication January 4, 2021, date of current version January 13, 2021.

Digital Object Identifier 10.1109/ACCESS.2020.3048941

More Efficient AC Filterless Flexible LCC HVDC by Analyzing the Impact of Single-Phase Fault on Commutations

CONGHUAN YANG, YING XUE, (Member, IEEE), AND XIAO-PING ZHANG, (Fellow, IEEE)
Department of Electronic, Electrical and Systems Engineering, University of Birmingham, Birmingham B15 2TT, U.K.

Corresponding author: Xiao-Ping Zhang (x.p.zhang@bham.ac.uk)

This work was supported in part by the Engineering and Physical Sciences Research Council (EPSRC) under Grant EP/N032888/1 and Grant EP/L017725/1.

ABSTRACT Single-phase fault is the most commonly occurred and severe AC fault that causes most of the Commutation Failures (CF) in LCC HVDC systems. It has long been regarded as having the same level of adverse impact on commutations of both 6-pulse bridges in the 12-pulse LCC HVDC scheme. This has resulted in the same level of investment on both 6-pulse bridges, for CF mitigation/elimination, e.g. firing angle advancement and equipment investment. However, due to different winding configurations of converter transformers, single-phase fault actually affects each 6-pulse bridge to different degrees. Based on the previously proposed AC Filterless Flexible LCC HVDC, this paper shows that, compared with the Y-Y bridge, the Y-Δ bridge has much smaller undesired phase advancement of the actual commutation voltage (commutation voltage at secondary side of converter transformer) under severe single-phase fault. As a result, the required voltage rating of controllable capacitors for Y-Δ bridge can be reduced, leading to considerable savings from reduced equipment costs and lower losses of controllable capacitors without compromising the commutation performance. The detailed theoretical analysis in this paper provides a valuable foundation for the development of more efficient CF mitigation/elimination strategies. Simulation results of 1) CIGRE HVDC benchmark system and 2) the same benchmark system but connected to a 39-bus inverter AC network are presented to validate the correctness of the analysis.

INDEX TERMS Commutation failure, LCC HVDC, single-phase fault.

I. INTRODUCTION

Mitigating or eliminating Commutation Failure (CF) in LCC HVDC systems has always been a significant technical challenge. It is even more challenging to achieve it in a way that is both technically and economically efficient. In the previously proposed AC Filterless Flexible LCC HVDC system [1], CF can be eliminated with 50% reduction of the required voltage rating of controllable capacitors, compared with that in the HVDC system proposed in [2]. For both HVDC systems, the voltage rating of controllable capacitor is determined by the required level of voltage insertion for CF elimination under single-phase fault. It is because the undesired phase shift in commutation voltage introduced by single-phase fault considerably increases the required insertion voltage level [2]. The same voltage rating of controllable capacitors is applied to both 6-pulse bridges of a 12-pulse scheme in previous methods.

The associate editor coordinating the review of this manuscript and approving it for publication was Dragan Jovcic.

However as the winding configurations of converter transformers are different for the two 6-pulse bridges (one connected in Y-Y and the other in Y-Δ [3]), the impact of single-phase fault on the phase shift of actual commutation voltage (commutation voltage at secondary side of converter transformer for AC Filterless Flexible LCC HVDC [1]) are also different. As a result, the required voltage ratings of controllable capacitors for Y-Y and Y-Δ bridges are not necessarily the same. It provides an attractive opportunity to reduce the required voltage rating of controllable capacitors, hence the associated costs and losses. Therefore the focus of this paper is, for the first time to the best of authors' knowledge, to analyze and exploit this potential to develop more efficient methods for CF elimination. The key contributions of this paper are

- For the first time, this paper develops a detailed theoretical analysis of the impact that single-phase fault has on phase shifts of actual commutation voltages. This has been neglected in previous studies [4]–[11] where zero

phase shifts in un-faulted phases are assumed. However in reality, the voltages of un-faulted phases will change in both magnitude and phase angle due to the zero sequence current from Y-Δ transformer. This is of direct practical importance to the operation of LCC HVDC systems as most of the CFs are caused by single-phase fault [4] which accounts for most of the power system faults. It opens up research opportunities in developing more effective methods in addressing CFs.

- Achievement of economic saving (estimated at M €3.69 as detailed in Section III.E) without compromising the commutation performance, comparing with AC Filterless Flexible LCC HVDC where the same voltage rating is applied for both Y-Y and Y-Δ bridges.

The performance of LCC HVDC system under unbalanced network conditions was analyzed in [12]–[16] where most of the research focused on the analysis of harmonics resulting from AC network unbalance. Limited considerations were given to unbalanced fault and its implications on CF. The impact of single-phase fault on CF in conventional LCC HVDC system was recognized in [4], [5] and briefly analyzed in [6] where it was pointed out that the commutation performances of two 6-pulse bridges are different under single-phase fault. However the analysis was based on the assumption of an infinite AC system where the voltage magnitude and phase angle of un-faulted phases are the same as pre-fault values, and the results are obtained with the valve groups blocked and open circuited. In reality, the voltages of un-faulted phases will change in both magnitude and phase angle due to zero sequence current from Y-Δ transformer, and the currents from valve side will also affect the phase shift of commutation voltage. These two aspects have direct impacts on the commutation performance. While the difference of commutation performance of two 6-pulse bridges under single-phase fault is recognized, limited further developments were made in exploiting it. On the other hand, the difference of impacts on CF between single-phase fault and three-phase fault was exploited in existing research for CF mitigation [17]–[19]. The advancement of firing angle upon detection of AC fault, as one of the most widely used methods for CF mitigation, distinguishes single-phase fault and three-phase fault by using different calculation methods. The calculated firing angle advancement was then applied to both 6-pulse bridges without distinguishing the difference of impacts from converter transformers. It is because the benefit of applying different firing angle advancements to the two bridges is limited for conventional LCC HVDC as the success of commutation is dominated by the level of voltage reduction and the commutation overlap.

In contrast to conventional LCC HVDC, AC Filterless Flexible LCC HVDC [1] exhibits fundamentally different behaviors. These behaviors make it much more beneficial by taking advantage of the different impacts from single-phase fault on two 6-pulse bridges. Firstly, the commutation is much faster in AC Filterless Flexible LCC HVDC [1]. This means that the commutation is much more sensitive to the phase shift than the commutation voltage magnitude. Secondly, the driving voltage for commutation becomes the voltage at the secondary side of converter transformer (i.e., the actual commutation voltage). Therefore a positive actual commutation voltage, even with relatively small magnitude can lead to successful commutations. On the contrary, the same level of positive commutation voltage will cause CF in conventional LCC HVDC as a much larger commutation overlap will infringe upon the available extinction angle. It will be shown in this paper that in AC Filterless Flexible LCC HVDC, the Y-Δ bridge is less prone to CF than Y-Y bridge especially under severe single-phase fault. Consequently the voltage rating of controllable capacitors for Y-Δ bridge can be reduced without compromising the commutation performance.

The rest of the paper is organized as follows. Section II briefly reviews the AC Filterless Flexible LCC HVDC. Section III theoretically analyzes how actual commutation voltage in AC Filterless Flexible LCC HVDC is affected by single-phase fault. Section IV presents the simulation results of balanced and unbalanced faults to validate the effectiveness of the proposed method. Discussions with respect to practical applications are also included. Finally Section V concludes the paper.

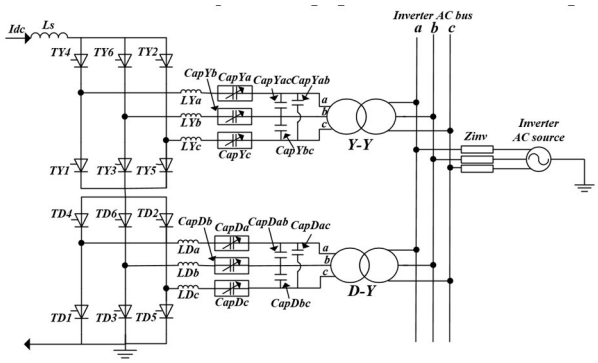

FIGURE 1. Circuit configuration of AC Filterless Flexible LCC HVDC.

II. AC FILTERLESS FLEXIBLE LCC HVDC

Fig. 1 shows the circuit configuration of AC Filterless Flexible LCC HVDC system where I_{dc} is the DC current; *TY(D)1-TY(D)6* are thyristor valves; *LY(D)a-LY(D)c* and *CapY(D)a-CapY(D)c* are current limiting inductors and controllable capacitors respectively; *CapY(D)ab*, *CapY(D)bc* and *CapY(D)ac* are parallel capacitors; Z_{inv} is the AC network impedance. With reference to Fig. 1, the functionalities of the main components are (more details are shown in [1]): The controllable capacitors provide the essential extra commutation voltage to guarantee the success of commutations. The same voltage rating, determined by the level of insertion voltage required to eliminate CF under single-phase fault, is adopted for controllable capacitors connected to both Y-Y and Y-Δ bridges. The parallel capacitors 1) reduce the filtering requirement of AC harmonics and 2) increase the speed of

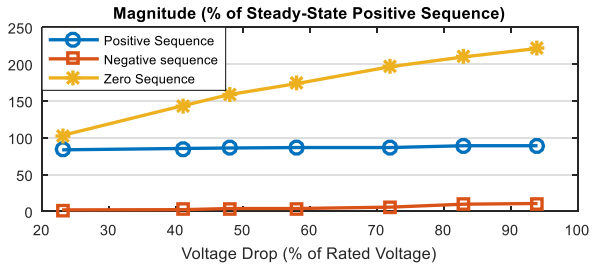

FIGURE 2. Magnitudes of sequence components under single-phase fault.

commutation so that it no longer depends on the commutation reactance (largely the reactance from converter transformers). The current limiting inductors help control the commutation speed. The objectives of this paper are to analyze in detail the impact of single-phase fault on each of the 6-pulse bridges, and reduce the requirement of voltage insertion from controllable capacitors without adding extra equipment or control complexity.

III. COMMUTATION PERFORMANCE UNDER SINGLE-PHASE FAULT

There are three aspects to be considered when analyzing the actual commutation voltage under single-phase fault: 1) representation of inverter; 2) transformer connection and 3) AC network. All three aspects are discussed in this section.

A. REPRESENTATION OF INVERTER

During single-phase fault, both 6-pulse bridges are injecting fault current into the AC network. The total injected fault current consists of positive, negative and zero sequence components. However, as mentioned in [6], a detailed representation of the valve behavior during unbalanced fault is difficult and simplifications are needed herein.

Fig. 2 shows the magnitudes of positive, negative and zero sequence components of fault current from inverter during single-phase fault. Different levels of voltage drop are simulated using the AC Filterless Flexible LCC HVDC modified from HVDC Benchmark system [1]. The magnitudes of fault current sequence components are expressed as percentages of the rated inverter AC current, which means that under the rated condition, the magnitude of positive sequence is 100% and the magnitudes of negative and zero sequence are 0%. It can be seen from Fig. 2 that for different levels of voltage drop, the positive sequence component is only reduced to 85-90%, and the level of negative sequence component is small (less than 10%). In contrast, the zero sequence current is experiencing a significant increase with the largest magnitude among all three sequence components. The positive and negative sequence currents are from the valve side (i.e., current flowing through current limiting inductors) and the 'transformer-parallel capacitor' part of the circuit under unbalanced fault. Zero sequence current is generated from the Y-Δ transformer under unbalanced fault.

In terms of impact on actual commutation voltage, the large zero sequence current contributes significantly to the change of actual commutation voltage, which is neglected in previous studies. It flows through the un-faulted phases into the network causing additional change of voltages in those phases and this in turn affects the actual commutation voltage. On the other hand, contribution from negative sequence current is small due to its much smaller magnitude. Therefore to simplify the analysis, negative sequence current from the valve side during single-phase fault will be neglected in the following analysis. Simulation results in Section IV also show that the calculation error due to this negligence is small.

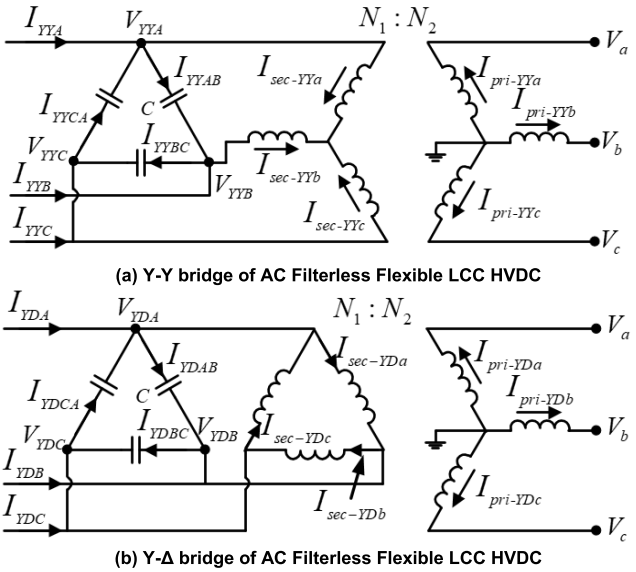

FIGURE 3. Configurations of two 6-pulse bridges of AC Filterless Flexible LCC HVDC.

B. TRANSFORMER CONNECTION

Fig. 3 shows the circuit diagrams for two 6-pulse bridges of AC Filterless Flexible LCC HVDC where $I_{YY(D)A}$-$I_{YY(D)C}$ are currents from the valve side; $I_{YY(D)AB}$, $I_{YY(D)BC}$, $I_{YY(D)CA}$ are currents through parallel capacitors; $I_{sec-YY(D)a}$-$I_{sec-YY(D)c}$ are currents at secondary side of converter transformers; $I_{pri-YY(D)a}$-$I_{pri-YY(D)c}$ are currents at primary side of converter transformers; $V_{YY(D)A}$-$V_{YY(D)C}$ are phase voltages at secondary sides; V_a-V_c are primary side voltages; N_1: N_2 is the transformer turns ratio. The positive directions of the currents are shown in the figure. Based on Fig. 3, the actual commutation voltages under single-phase fault can be calculated where the impact from zero sequence current is inherently considered. The calculation results will then be used to determine the required level of voltage insertion from controllable capacitors for Y-Δ bridge.

For Y-Y bridge, as shown in Fig. 3(a), the following circuit equations can be written:

$$I_{sec-YYa} = I_{YYA} + I_{YYCA} - I_{YYAB} \quad (1)$$

$$I_{sec-YYb} = I_{YYB} + I_{YYAB} - I_{YYBC} \quad (2)$$

$$I_{sec-YYc} = I_{YYC} + I_{YYBC} - I_{YYCA} \tag{3}$$

The currents through parallel capacitors can be calculated using the primary side AC voltages:

$$I_{YYAB} = \frac{V_{YYAB}}{\left(1/j\omega C\right)} = \frac{\left(V_a - V_b\right)\left(N_1/N_2\right) + jX_L\left(I_{sec-YYa} - I_{sec-YYb}\right)}{\left(1/j\omega C\right)} \tag{4}$$

$$I_{YYBC} = \frac{V_{YYBC}}{\left(1/j\omega C\right)} = \frac{\left(V_b - V_c\right)\left(N_1/N_2\right) + jX_L\left(I_{sec-YYb} - I_{sec-YYc}\right)}{\left(1/j\omega C\right)} \tag{5}$$

$$I_{YYCA} = \frac{V_{YYCA}}{\left(1/j\omega C\right)} = \frac{\left(V_c - V_a\right)\left(N_1/N_2\right) + jX_L\left(I_{sec-YYc} - I_{sec-YYa}\right)}{\left(1/j\omega C\right)} \tag{6}$$

where C and X_L are capacitance of parallel capacitors and reactance of converter transformer and

$$V_{YYAB} = V_{YYA} - V_{YYB}, \quad V_{YYBC} = V_{YYB} - V_{YYC}, \quad V_{YYCA} = V_{YYC} - V_{YYA} \tag{7}$$

are the actual commutation voltages for Y-Y bridge. By substituting (4)-(6) into (1)-(3), the secondary side winding currents for Y-Y bridge can be calculated as:

$$I_{sec-YYa} = \left(A_1 + I_{YYA}\right)/\left(1 - 3\omega X_L C\right) \tag{8}$$

$$I_{sec-YYb} = \left(A_2 + I_{YYB}\right)/\left(1 - 3\omega X_L C\right) \tag{9}$$

$$I_{sec-YYc} = \left(A_3 + I_{YYC}\right)/\left(1 - 3\omega X_L C\right) \tag{10}$$

where

$$A_1 = \left(V_c - 2V_a + V_b\right) \times \left(N_1/N_2\right) \times j\omega C \tag{11}$$

$$A_2 = \left(V_a - 2V_b + V_c\right) \times \left(N_1/N_2\right) \times j\omega C \tag{12}$$

$$A_3 = \left(V_b - 2V_c + V_a\right) \times \left(N_1/N_2\right) \times j\omega C \tag{13}$$

Similarly circuit equations can be written for Y-Δ bridge:

$$I_{YDA} + I_{YDCA} + I_{sec-YDc} = I_{YDAB} + I_{sec-YDa} \tag{14}$$

$$I_{YDB} + I_{YDAB} + I_{sec-YDa} = I_{YDBC} + I_{sec-YDb} \tag{15}$$

$$I_{YDC} + I_{YDBC} + I_{sec-YDb} = I_{YDCA} + I_{sec-YDc} \tag{16}$$

The currents through parallel capacitors can also be calculated using the primary side AC voltages:

$$I_{YDAB} = \frac{V_{YDAB}}{\left(1/j\omega C\right)} = \frac{\sqrt{3}V_a \times \left(N_1/N_2\right) + 3jX_L I_{sec-YDa}}{\left(1/j\omega C\right)} \tag{17}$$

$$I_{YDBC} = \frac{V_{YDBC}}{\left(1/j\omega C\right)} = \frac{\sqrt{3}V_b \times \left(N_1/N_2\right) + 3jX_L I_{sec-YDb}}{\left(1/j\omega C\right)} \tag{18}$$

$$I_{YDCA} = \frac{V_{YDCA}}{\left(1/j\omega C\right)} = \frac{\sqrt{3}V_c \times \left(N_1/N_2\right) + 3jX_L I_{sec-YDc}}{\left(1/j\omega C\right)} \tag{19}$$

where

$$V_{YDAB} = V_{YDA} - V_{YDB}, \quad V_{YDBC} = V_{YDB} - V_{YDC}, \quad V_{YDCA} = V_{YDC} - V_{YDA} \tag{20}$$

are the actual commutation voltages for Y-Δ bridge. By substituting (17)-(19) into (14)-(16) and considering that

$$V_{YDAB} + V_{YDBC} + V_{YDCA} = 0 \tag{21}$$

the secondary side winding currents can be calculated as:

$$I_{sec-YDa} = \frac{3K_1K_2V_a + K_1\left(V_a + V_b + V_c\right) + K_2\left(I_{YDB} - I_{YDA}\right)}{-3\left(K_2 + 1\right)K_2} \tag{22}$$

$$I_{sec-YDb} = \frac{3K_1K_2V_b + K_1\left(V_a + V_b + V_c\right) + K_2\left(I_{YDC} - I_{YDB}\right)}{-3\left(K_2 + 1\right)K_2} \tag{23}$$

$$I_{sec-YDc} = \frac{3K_1K_2V_c + K_1\left(V_a + V_b + V_c\right) + K_2\left(I_{YDA} - I_{YDC}\right)}{-3\left(K_2 + 1\right)K_2} \tag{24}$$

where $K_1 = \sqrt{3}j\omega C \times \left(N_1/N_2\right)$, $K_2 = -3\omega X_L C$. To calculate the actual commutation voltages during fault, the changes of primary side AC voltages need to be calculated. As an example considering a Phase A fault, the changes of primary side voltages of Phase B and Phase C can be expressed as:

$$\Delta V_b = Z_{sys} \times \left(\left(I_{pri-YYb} + I_{pri-YDb}\right) - \left(I^{fault}_{pri-YYb} + I^{fault}_{pri-YYb}\right)\right) \tag{25}$$

$$\Delta V_c = Z_{sys} \times \left(\left(I_{pri-YYc} + I_{pri-YDc}\right) - \left(I^{fault}_{pri-YYc} + I^{fault}_{pri-YYc}\right)\right) \tag{26}$$

where the superscript '*fault*' represents the variables during fault; 'Δ' represents the difference of variables between pre-fault and fault conditions (i.e., $\Delta V_b = V_b - V_b^{fault}$); Z_{sys} represents the impedance seen by the current in healthy phases during fault, which will be discussed in *Subsection C*. By substituting (8)-(10) and (22)-(24) (for both fault and pre-fault conditions) into (25)-(26), ΔV_b and ΔV_c can be calculated as:

$$\Delta V_b = \frac{-\left(D + 1\right)E - F \times B - \left(B^2 + BD + B\right)\Delta V_a}{B^2 - D^2 - 2D - 1} \tag{27}$$

$$\Delta V_c = \frac{-E \times B - F\left(D + 1\right) - \left(B^2 + BD + B\right)\Delta V_a}{B^2 - D^2 - 2D - 1} \tag{28}$$

where

$$B = j\omega C\left(\frac{N_1}{N_2}\right)^2 \times \frac{Z_{sys}}{1 - 3\omega X_L C} \times \frac{K_2 - 1}{K_2}, D = B\frac{5K_2 + 1}{K_2 - 1} \tag{29}$$

$$E = Z_{sys}\left(\frac{\Delta I_{YYB}}{1-3\omega X_L C}\frac{N_1}{N_2} + \sqrt{3}\frac{N_1}{N_2}\frac{\Delta I_{YDC}-\Delta I_{YDB}}{-3\left(K_2+1\right)}\right) \tag{30}$$

$$F = Z_{sys}\left(\frac{\Delta I_{YYC}}{1-3\omega X_L C}\frac{N_1}{N_2} + \sqrt{3}\frac{N_1}{N_2}\frac{\Delta I_{YDA}-\Delta I_{YDC}}{-3\left(K_2+1\right)}\right) \tag{31}$$

Using (27)-(28), the Phase B and Phase C voltages during fault can be calculated. Together with the expressions of (4)-(6) and (8)-(10) under fault (with superscript '*fault*'), the actual commutation voltages for Y-Y bridge can be calculated as:

$$V_{YYAB}^{fault} = V_{ab}^{fault} \times \frac{N_1}{N_2\left(1-3\omega X_L C\right)} + \frac{jX_L\left(I_{YYA}^{fault}-I_{YYB}^{fault}\right)}{1-3\omega X_L C} \tag{32}$$

$$V_{YYBC}^{fault} = V_{bc}^{fault} \times \frac{N_1}{N_2\left(1-3\omega X_L C\right)} + \frac{jX_L\left(I_{YYB}^{fault}-I_{YYC}^{fault}\right)}{1-3\omega X_L C} \tag{33}$$

$$V_{YYCA}^{fault} = V_{ca}^{fault} \times \frac{N_1}{N_2\left(1-3\omega X_L C\right)} + \frac{jX_L\left(I_{YYC}^{fault}-I_{YYA}^{fault}\right)}{1-3\omega X_L C} \tag{34}$$

where

$$\begin{aligned} V_{ab}^{fault} &= V_a^{fault} - V_b^{fault} \\ V_{bc}^{fault} &= V_b^{fault} - V_c^{fault} \\ V_{ca}^{fault} &= V_c^{fault} - V_a^{fault} \end{aligned} \tag{35}$$

Similarly for Y-Δ bridge, equations of (22)-(24) under fault are utilized together with (27)-(28) to calculate the secondary side currents, which are further substituted into (17)-(19) to calculate the actual commutation voltages during fault:

$$\begin{aligned} V_{YDAB}^{fault} = {} & \sqrt{3}V_a^{fault}\frac{N_1}{N_2} - jX_L\frac{3K_1V_a^{fault}}{\left(1+K_2\right)} \\ & + jX_L\frac{K_1\left(V_a^{fault}+V_b^{fault}+V_c^{fault}\right)+K_2\left(I_{YDB}^{fault}-I_{YDA}^{fault}\right)}{-K_2\left(1+K_2\right)} \end{aligned} \tag{36}$$

$$\begin{aligned} V_{YDBC}^{fault} = {} & \sqrt{3}V_b^{fault}\frac{N_1}{N_2} - jX_L\frac{3K_1V_b^{fault}}{\left(1+K_2\right)} \\ & + jX_L\frac{K_1\left(V_a^{fault}+V_b^{fault}+V_c^{fault}\right)+K_2\left(I_{YDC}^{fault}-I_{YDB}^{fault}\right)}{-K_2\left(1+K_2\right)} \end{aligned} \tag{37}$$

$$\begin{aligned} V_{YDCA}^{fault} = {} & \sqrt{3}V_c^{fault}\frac{N_1}{N_2} - jX_L\frac{3K_1V_c^{fault}}{\left(1+K_2\right)} \\ & + jX_L\frac{K_1\left(V_a^{fault}+V_b^{fault}+V_c^{fault}\right)+K_2\left(I_{YDA}^{fault}-I_{YDC}^{fault}\right)}{-K_2\left(1+K_2\right)} \end{aligned} \tag{38}$$

Equations (32)-(38) will be used in *Subsection D* to calculate the phase shifts of actual commutation voltages for Y-Y and Y-Δ bridges, and in *Subsection E* to estimate the required voltage rating for Y-Δ bridge. The zero sequence current in the secondary winding of Y-Δ converter transformer can be calculated as

$$\begin{aligned} I_{sec-YDzero}^{fault} &= I_{sec-YDa}^{fault} + I_{sec-YDb}^{fault} + I_{sec-YDc}^{fault} \\ &= \left(V_a^{fault} + V_b^{fault} + V_c^{fault}\right) \times \left(-K_1/K_2\right) \end{aligned} \tag{39}$$

It can be seen from (39) that zero sequence current is generated by voltage unbalance applied across the equivalent winding reactance. With a more severe unbalance fault, i.e., higher level of unbalance, the zero sequence current will be higher.

C. AC NETWORK

The AC network affects the actual commutation voltage through Z_{sys} as seen from (27)-(28). Z_{sys} is affected by system operating condition and network topology. In practice, as the value of Z_{sys} will change due to a change of operating condition or network topology, simulation studies can be carried out to determine the range of Z_{sys} under which the inverter may operate. The impact of Z_{sys} on the phase shift of actual commutation voltage (which determines the required voltage rating of controllable capacitors for CF elimination) is discussed in detail in the following section.

D. NUMERICAL EXAMPLE

In this section, the phase advancements of actual commutation voltages under single-phase fault are calculated using equations derived in *Subsection B*. The impact from varying network impedance is also analyzed. Phase A fault is considered as an example and the parameters from Benchmark system (where Z_{sys} is equal to the positive sequence impedance of the inverter AC network) are used [20]. Negative phase-angle jump (the during-fault voltage is lagging the pre-fault voltage) is considered for Phase A voltage during fault due to the direction of power flow. Detailed studies related to phase-angle jump can be found in [21], [22].

The calculation results are shown in Fig. 4 and Fig. 5. Fig. 4 shows the phase advancements of actual commutation voltages under different levels of voltage drop (10%, 40%, 80%) and phase-angle jumps (−70 degree to 0 degree). Fig. 5 shows the impact of network impedance (Z_{sys}, 50%∗Z_{sys}, 150%∗Z_{sys}) on the phase advancements of actual commutation voltages. In Fig. 5, three curves highlighted by each circle correspond to three different network impedance under a specific voltage drop (i.e., 10%, 40% or 80% as indicated in Fig. 5). From Fig. 4 and Fig. 5, the following observations can be made:

- The actual commutation voltages of V_{YYCA} and V_{YDCA} are experiencing a phase delay (negative phase advancements) during the fault as shown in Fig. 4(c). The level of phase delay is considerable (in particular for faults with larger negative phase-angle jumps) which is beneficial for commutations and will have limited impact on required voltage rating of the controllable capacitors.

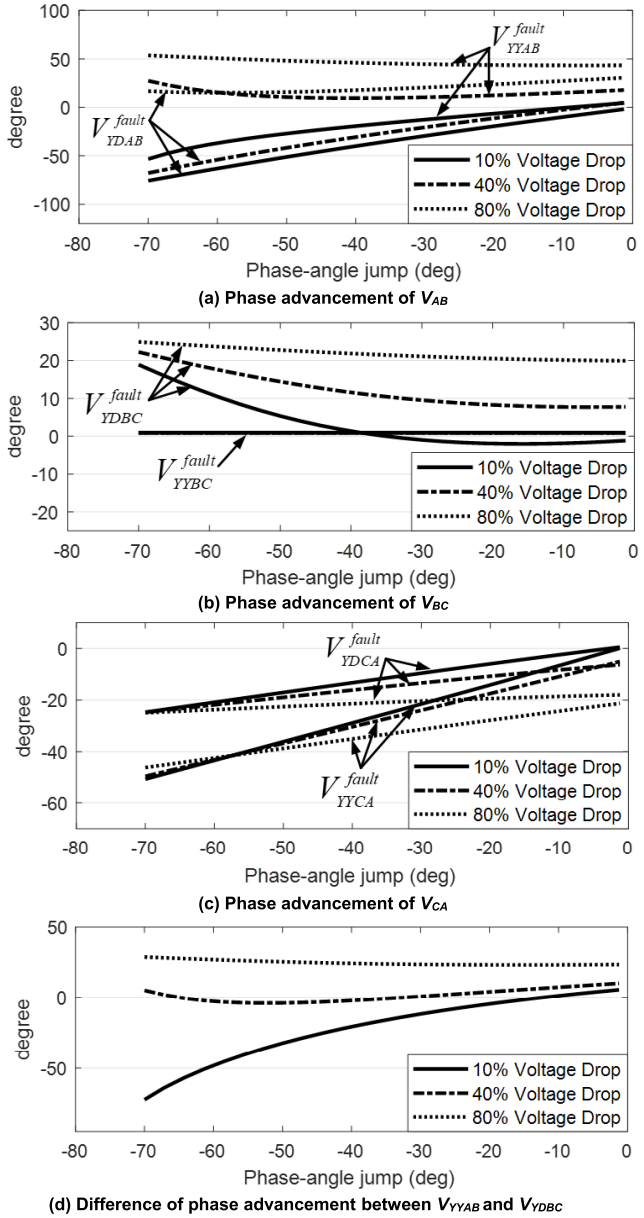

(a) Phase advancement of V_{AB}

(b) Phase advancement of V_{BC}

(c) Phase advancement of V_{CA}

(d) Difference of phase advancement between V_{YYAB} and V_{YDBC}

FIGURE 4. Phase advancements of actual commutation voltages with different levels of voltage drop.

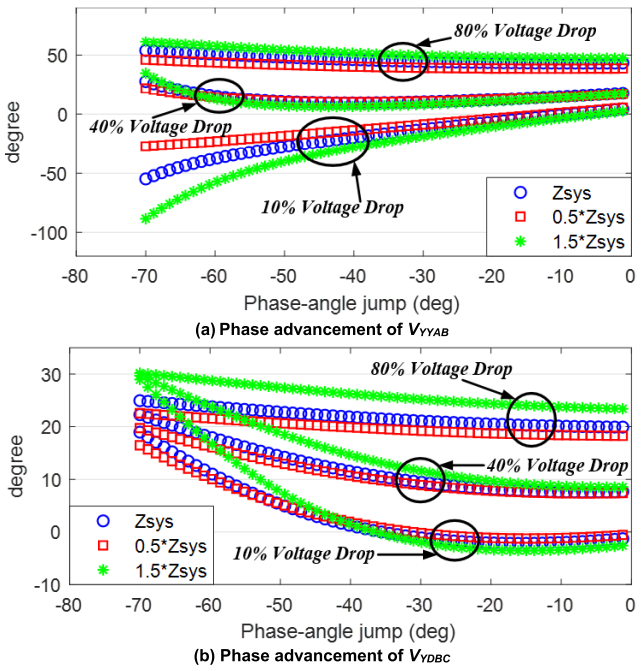

(a) Phase advancement of V_{YYAB}

(b) Phase advancement of V_{YDBC}

FIGURE 5. Impact of network impedance on phase advancements of actual commutation voltages.

- V_{YYAB} and V_{YDBC} may experience large positive phase advancements (Fig. 4(a) and Fig. 4(b)) under serious single-phase fault, and they tend to advance more with higher levels of voltage drop. So from the point of view of CF elimination, the phase advancements of V_{YYAB} and V_{YDBC} under the most serious single-phase faults will determine the required voltage ratings of controllable capacitors for Y-Y and Y-Δ bridges, respectively. To show the difference of phase advancement between V_{YYAB} and V_{YDBC}, Fig. 4(d) is plotted. From Fig. 4(d) it can be seen that the phase advancement of V_{YYAB} is much larger than that of V_{YDBC} under serious fault (dotted line in Fig. 4(d)). As mentioned earlier, the impact of this on CF is unlikely to be obvious in conventional LCC HVDC systems because the overlap angle is large at reduced commutation voltage, overshadowing the effect of difference in phase advancements. However the impact is significant for AC Filterless Flexible LCC HVDC as it has much smaller overlap angle and is less dependent on the magnitude of commutation voltage. As a result, the required voltage rating of controllable capacitor for Y-Δ bridge can be lower than that of Y-Y bridge, rather than identical as previously adopted in [1].
- The change of AC network impedance has limited impact on the phase advancements of actual commutation voltages as shown in Fig. 5. The impact is slightly higher for V_{YDBC} when the fault is severe but the phase advancement is still much less than that of V_{YYAB}. This is beneficial as it means that a lower voltage rating of controllable capacitor for Y-Δ bridge adopted for a particular network condition can maintain commutation performance when network condition changes. This is further verified through simulation studies in *Section IV* for AC Filterless Flexible LCC HVDC connected to a 39-bus system where the voltage rating of Y-Δ is determined using the Benchmark network impedance.

To better explain the calculation results, Fig. 6 shows the phasor diagrams of electrical variables for Y-Y and Y-Δ bridges under Phase A fault. The actual commutation voltages of V_{YYAB} and V_{YDBC} during fault are shown as they have the largest phase advancements in Y-Y and Y-Δ bridges.

For Y-Y bridge as shown in Fig. 6(a), it can be seen that the phase advancement of V_{YYAB} is affected by two factors. Firstly, V_b is advanced by ΔV_b (resulting mainly from zero sequence fault current flowing into the AC network).

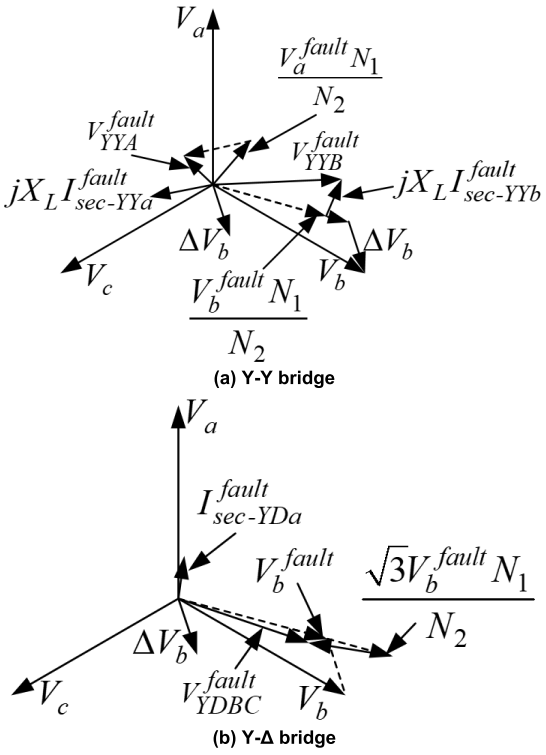

FIGURE 6. Phasor diagrams of main electrical variables for both bridges.

Secondly, V_a^{fault} and V_b^{fault} are advanced in phase because of the voltage drop across transformer reactance to get V_{YYA}^{fault} and V_{YYB}^{fault}. It can also be seen from Fig. 6(a) that the above two factors are increasing the phase advancement of V_{YYAB}^{fault}.

On the other hand for Y-Δ bridge as shown in Fig. 6(b), it can be seen that the main source of phase advancement of V_{YDBC} is from ΔV_b. Unlike Y-Y bridge, the voltage drop across the transformer reactance leads to additional phase delay in V_{YDBC}^{fault}. Therefore the net result is a much smaller phase advancement in V_{YDBC}^{fault} compared with that of V_{YYAB}^{fault}.

Although Fig. 6 shows the phasor relationships under a particular condition, these relationships hold true for a range of fault and network conditions according to the calculation results shown in Fig. 4 and Fig. 5.

E. VOLTAGE RATING OF CONTROLLABLE CAPACITORS

To estimate the required voltage rating of controllable capacitors for Y-Y and Y-Δ bridges considering the difference of phase advancements in actual commutation voltages, Fig. 7 is drawn for illustration. In Fig. 7, α represents the firing instant for actual commutation voltage, μ_{max} represents the maximum commutation overlap angle and β represents the phase advancements of actual commutation voltages during fault. β for different actual commutation voltages are calculated according to (32)-(38). It can be clearly seen from Fig. 7 that the actual commutation voltage becomes negative because of the phase advancements. As a result the voltage insertion from controllable capacitors are needed to guarantee

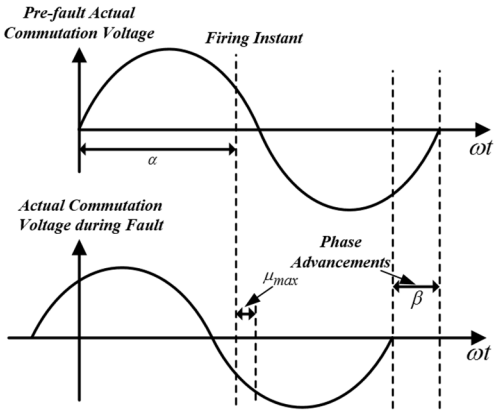

FIGURE 7. Effect of fault on actual commutation voltage.

the success of commutations. The larger the phase advancement is, the higher the voltage insertion is required from the controllable capacitors. Considering the same Phase A fault, the required voltage insertion from controllable capacitors in each phase for Y-Y bridge can be estimated as (with reference to Fig. 7):

$$V_{YYCap} = \left|\sqrt{2}V_{YYAB}^{fault}\sin\left(\alpha + \beta_{YYAB} + \mu_{max}\right)\right| \Big/ 2 \quad (40)$$

where β_{YYAB} is the phase advancement of V_{YYAB} during fault. V_{YYAB} is used in the calculation as it has the largest phase advancements during Phase A fault as discussed in the last section. Similarly for Y-Δ bridge, the required voltage rating from controllable capacitors can be estimated as:

$$V_{YDCap} = \left|\sqrt{2}V_{YDBC}^{fault}\sin\left(\alpha + \beta_{YDBC} + \mu_{max}\right)\right| \Big/ 2 \quad (41)$$

where β_{YDBC} is the phase advancement of V_{YDBC} during fault. As an example, when a firing angle of 162^0 and a maximum overlap angle of 10^0 [1] are considered (note that the increased DC current during fault is taken into account by considering a larger overlap angle), the phase advancements of V_{YYAB} (i.e., β_{YYAB}) and V_{YDBC} (β_{YDBC}) can be calculated to be 50.3^0 and 23.5^0 respectively under phase A fault with 80% of voltage drop (the same calculation applies for different levels of voltage drop). Then the required voltage rating of controllable capacitors can be estimated as 54.7kV for Y-Y bridge and 41.6kV for Y-Δ bridge. Due to the fact that the initial transients of actual commutation voltages during unbalanced faults are also affecting the commutation performance, simulation studies are carried out to determine the final values of voltage rating, which are 60kV and 45kV for Y-Y and Y-Δ bridges respectively. In practice, simulation studies are needed to fine tune the calculated voltage rating of controllable capacitors. For the system considered in this paper, the end result is a reduction of 15kV (60kV to 45kV) for Y-Δ bridge, leading to direct reductions of equipment cost and capitalized cost of losses from controllable capacitors.

Table 1 shows the comparison of cost of controllable capacitors between the AC Filterless Flexible LCC HVDC [1] and the proposed method. It can be seen from Table 1 that

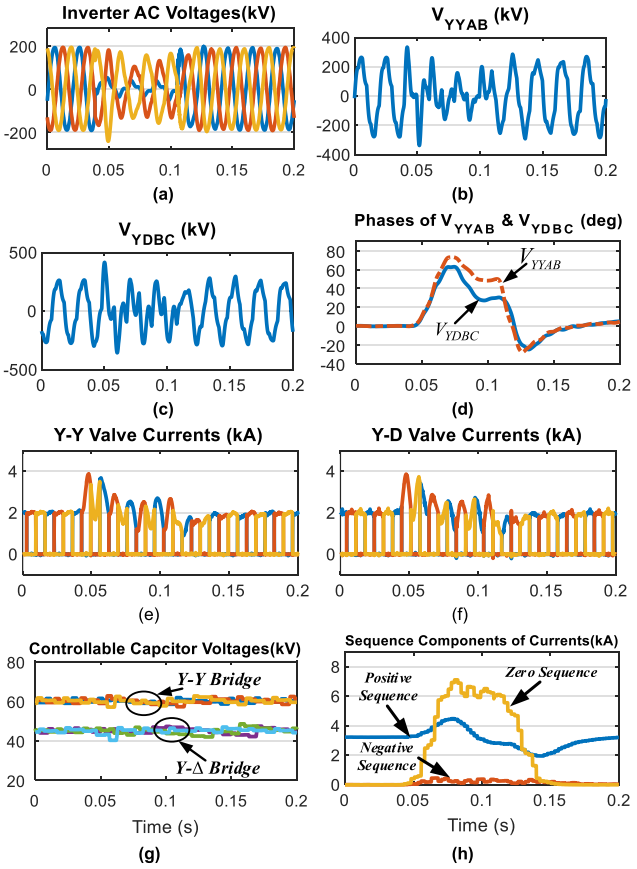

FIGURE 8. Single-phase fault when SCR = 2.5 with the proposed method.

the total saving is M€3.69 (M€29.58-M€25.89), which is attractive as the same commutation performance is achieved at lower cost. The equipment cost of controllable capacitors is estimated using the estimated cost of M€92.28 for full bridge valves of a ±525kV MMC [23]. For example for the proposed method, equipment cost is calculated as $\text{M€}(92.28 \times 105/525) = \text{M€}18.46$. The capitalized cost of losses is estimated using the 1) 2.2MW of losses from controllable capacitors rated at 140kV [2] and 2) evaluation of capitalized cost of losses at €4500 per kW [24]. For the proposed method it is calculated as $\text{M€}(2.2 \times 4.5 \times 105/140) = \text{M€}7.43$.

IV. SIMULATION RESULS

Two case studies are carried out in this section.

Case 1: Simulation results of single-phase fault and three-phase fault are presented to demonstrate the commutation performance with reduced voltage rating of controllable capacitors for Y-Δ bridge. Comparisons are made with AC Filterless Flexible LCC HVDC where the same voltage rating (60kV) of controllable capacitors is adopted for both Y-Y and Y-Δ bridges. The HVDC Benchmark system is modified by including the controllable capacitors and fixed parallel capacitors as shown in Fig. 1 where the system data is obtained from [20] and the parallel capacitance of 10 μF is used.

TABLE 1. Cost comparison of controllable capacitors.

	AC Filterless Flexible LCC HVDC	Proposed Method
Equipment cost	M€21.09	M€18.46
Capitalized cost of losses	M€8.49	M€7.43
Total	M€29.58	M€25.89
Percentage of reduction	0%	12.5%

In addition, to demonstrate the effectiveness of the proposed method under different SCR conditions, simulation results of single-phase fault using modified HVDC Benchmark system with a reduced SCR of 2 are presented. Reduced SCR is achieved by increasing the inverter side system impedance. SCR condition of 2 is regarded as very weak system [25]. Simulation results of a stronger system, i.e., SCR = 3.5 are presented in Case 2.

Case 2: This case is to demonstrate the robustness of the proposed method under a changing network condition. For this purpose, the same controllable capacitor rating as that in Case 1 (calculated using the HVDC benchmark system) is adopted, while a different inverter AC network, i.e., a 39-bus system [26] with detailed representations of transmission lines and synchronous generators is used.

A. SIMULATION RESULTS OF CASE 1

Fig. 8 shows the simulation results of a Phase A fault at inverter AC bus. During the fault, Phase A voltage is dropped by 80% as shown in Fig. 8(a) but the commutations are still successful in both Y-Y and Y-Δ bridges as shown in Fig. 8(e) and Fig. 8(f). This is achieved with Y-Δ bridge having 25% lower voltage rating of controllable capacitors than that in Y-Y bridge as shown in Fig. 8(g). The actual commutation voltages of V_{YYAB} and V_{YDBC} are experiencing magnitude drops (Fig. 8(b) and Fig. 8(c)) and unfavorable phase shifts as shown in Fig. 8(d) where positive values indicate phase advancements. It can be seen from Fig. 8(d) that V_{YDBC} has smaller phase advancement than V_{YYAB}. Further from Fig. 8(d), the measured phase advancements of V_{YYAB} and V_{YDBC} are 48.70^0 and 24.80^0 respectively, which match the calculated phase shifts of 50.30^0 and 23.50^0. Fig. 8(h) shows the sequence components of inverter current injection during fault. It can be seen that the zero sequence component increases significantly during the fault while the positive sequence component is increased at the beginning of the fault and then stabilizes at a value slightly below the steady-state one. The negative sequence component has a much smaller increase in magnitude during the fault.

In comparison with results in Fig. 8, Fig. 9 shows the simulation results using AC Filterless Flexible LCC HVDC where the same voltage rating of 60kV is adopted for Y-Y and Y-Δ bridges. As shown in Fig. 9(a), the same single-phase fault is simulated which causes an 80% voltage drop in Phase A. Similar to the results shown in Fig. 8, the actual commutation voltages of V_{YYAB} and V_{YDBC} are experiencing magnitude drops (Fig. 9(b) and Fig. 9(c)) and unfavorable phase shifts as shown in Fig. 9(d). Commutations are successful as shown

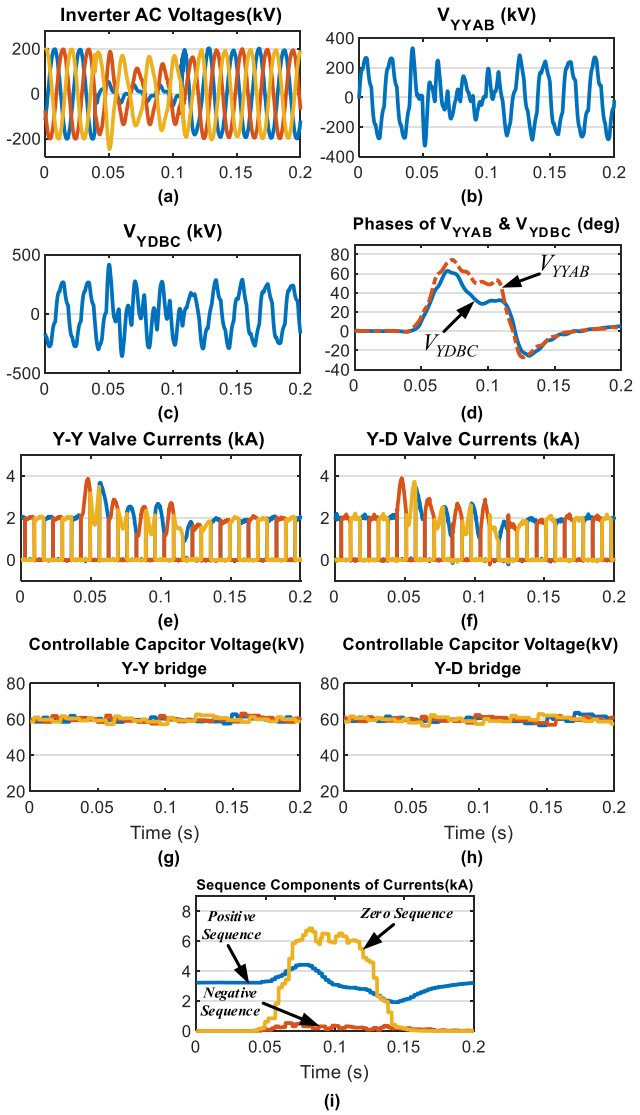

FIGURE 9. Single-phase fault using previously proposed AC Filterless Flexible LCC HVDC.

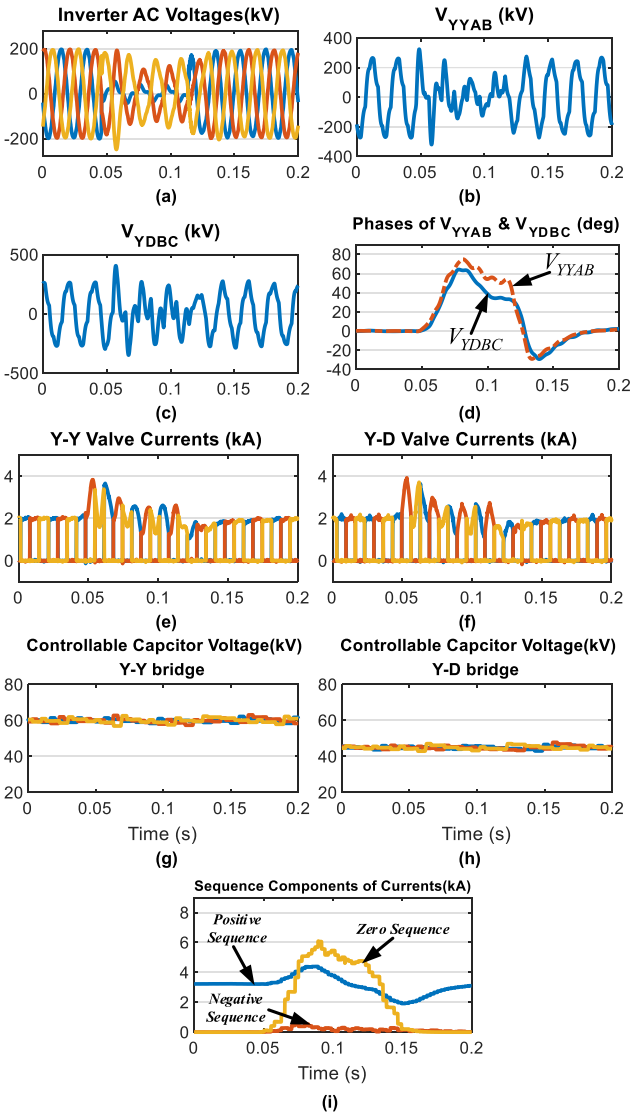

FIGURE 10. Single-phase fault when SCR = 2 with the proposed method.

in Fig. 9(e) and Fig. 9(f). These results are understandable as higher voltage rating of controllable capacitors for Y-Δ bridge only affects the speed of commutation (as they are inserted during the commutation period) with very limited impacts on actual commutation voltages. Due to the same reason, the sequence components of inverter current injection as shown in Fig. 9(i) are similar to those shown in Fig. 8(h). The voltages of controllable capacitors are controlled at their reference values of 60kV as shown in Fig. 9(g) and Fig. 9(h).

To demonstrate the performance of the proposed method under a different SCR condition, simulation results using a modified HVDC Benchmark system with SCR = 2 are shown in Fig. 10. Single-phase fault is simulated that causes a Phase A voltage drop of 80% (Fig. 10(a)). Similar to the results shown in Fig. 8, commutations are successful (Fig. 10(e) and Fig. 10(f)) using the proposed voltage rating of controllable capacitors (Fig. 10(g) and Fig. 10(h)). The changes of magnitude of actual commutation voltages (Fig. 10(b) and Fig. 10(c)) are similar to those shown in Fig. 8. In particular, the phase shifts of actual commutation voltages as shown in Fig. 10(d) are similar to that shown in Fig. 8(d) which validates the theoretical results in Section III.D. The main difference in simulation results caused by different SCRs can be observed by comparing Fig. 10(i) with Fig. 8(h). It can be seen that with a smaller SCR (Fig. 10(i)), the magnitude of zero sequence current becomes smaller. It is understandable as a smaller SCR indicates larger equivalent network impedance.

Fig. 11 shows the simulation results of a three-phase fault at inverter AC bus. It can be seen from Fig. 11(a) that the three-phase voltages are dropped by 80% during the fault which causes significant voltage drops in the actual commutation voltages (Fig. 11(b) and Fig. 11(c)). However it can be seen from Fig. 11(d) and Fig. 11(e) that the commutations in

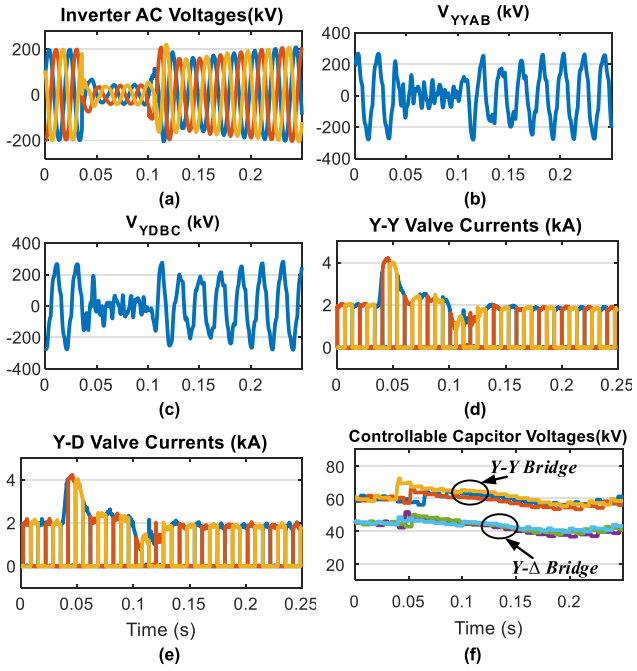

FIGURE 11. Three-phase fault with 80% voltage drop of the proposed method.

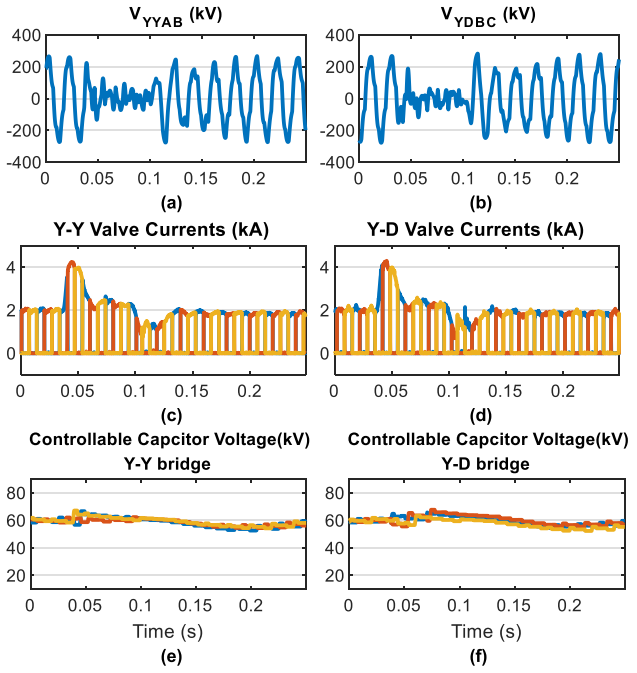

FIGURE 12. Three-phase fault with 80% voltage drop using previously proposed AC Filterless Flexible LCC HVDC.

both Y-Y and Y-Δ bridges are successful. With the significant decrease of actual commutation voltages, the commutations are now largely driven by the voltage from controllable capacitors.

As comparison, Fig. 12 shows the simulation results of the same fault as those shown in Fig. 11 but using AC Filterless Flexible LCC HVDC where the same voltage rating

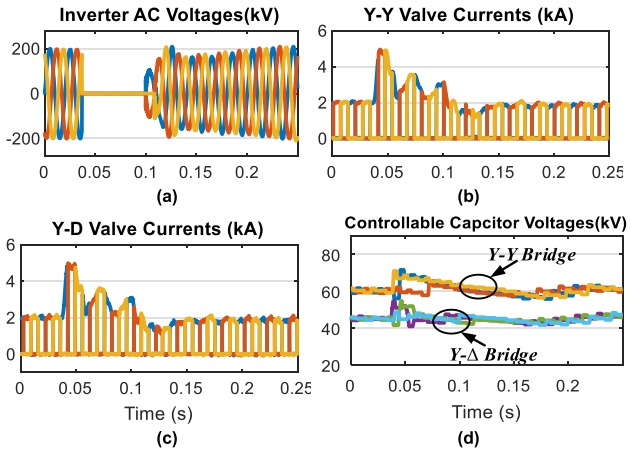

FIGURE 13. Three-phase fault with 100% voltage drop of the proposed method.

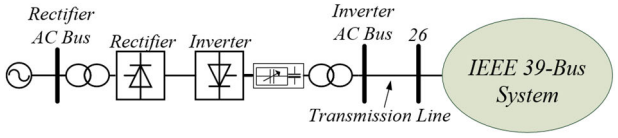

FIGURE 14. AC Filterless Flexible LCC HVDC connected to 39-bus AC system.

is adopted for both 6-pulse bridges. It can be seen from Fig. 12(c) and Fig. 12(d) that the commutations are successful. It is as expected because an increase of voltage rating of controllable capacitors for Y-Δ bridge contributes positively to the success of commutations. As discussed before, the increased voltage rating will have limited impact on the actual commutation voltages (Fig. 12(a) and Fig. 12(b)). Fig. 12(e) and Fig. 12(f) show that the voltages of controllable capacitors for both bridges are well controlled.

In fact for balanced fault, the commutations are still successful when the voltage drop is 100% (Fig. 13(a)) as shown in Fig. 13(b) and Fig. 13(c). This is because there are no significant phase advancements in actual commutation voltages under balanced fault so the required voltage insertion from controllable capacitors is less than that for single-phase fault.

B. SIMULATION RESULTS OF CASE 2

Fig. 14 shows the single-line diagram of the simulated system for Case 2 where the HVDC is connected to Bus 26 of the IEEE 39-bus system [26] through a transmission line. The inverter SCR is 3.5 (higher than the SCR = 2.5 and 2 simulated in Case 1). In addition, different from Case 1 where only the positive sequence Thevenin equivalent of the inverter AC system is considered, the detailed models of synchronous generators and transmission lines are simulated.

Fig. 15 shows the simulation results of the system under severe Phase A fault at inverter AC bus where the voltage is dropped by 80% (Fig. 15(a)). It can be seen from Fig. 15(e) and Fig. 15(f) that the commutations are successful. Similar to Case 1, the actual commutation voltages are experiencing drops in magnitude (Fig. 15(b) and Fig. 15(c)) and phase

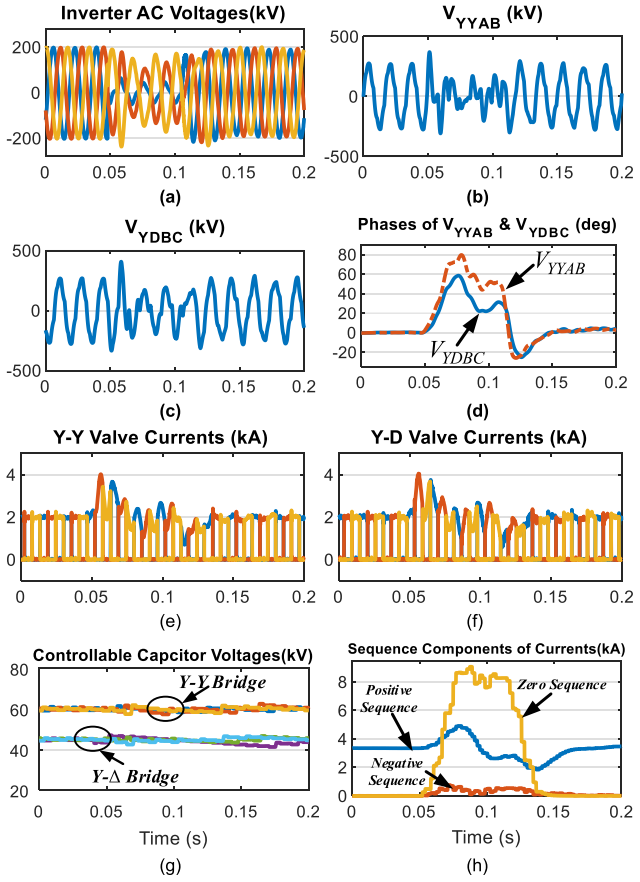

FIGURE 15. Single-phase fault for case 2 with the proposed method.

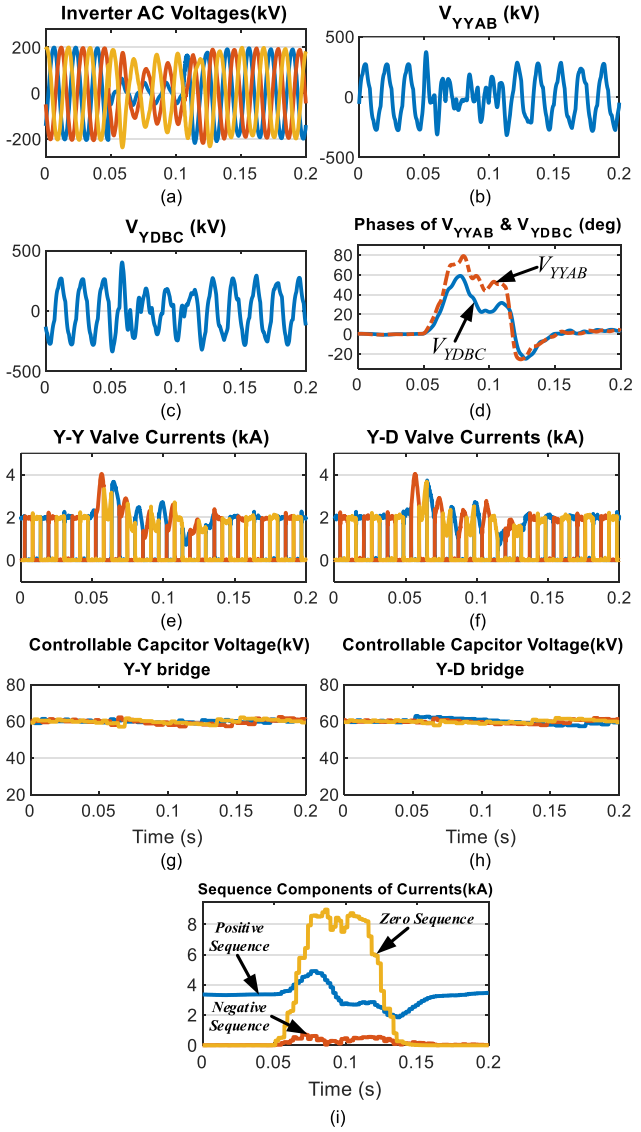

FIGURE 16. System responses under single-phase fault for case 2 using previously proposed AC Filterless Flexible LCC HVDC.

advancements (Fig. 15(d)). By comparing Fig. 15(d) with Fig. 8(d), it can be seen that the phase advancements in Case 2 for Y-Y and Y-Δ bridges are similar to those in Case 1, which agrees with the theoretical analysis in Section III. Same as Case 1, the elimination of CF is achieved with Y-Δ bridge having lower voltage rating than Y-Y bridge (Fig. 15(g)). From Fig. 15(h) it can be seen that the zero sequence current is significantly increased during the fault, similar to the results in Case 1.

As comparison, the same single-phase fault is applied but with AC Filterless Flexible LCC HVDC where the same voltage rating of controllable capacitors are adopted for both 6-pulse bridges. The simulation results are shown in Fig. 16. Fig. 16(a) shows that Phase A voltage is dropped by 80% but the commutations are successful (Fig. 16(e) and Fig. 16(f)). This is achieved with higher voltage ratings from controllable capacitors (Fig. 16(g) Fig. 16(h)). Similar to the results from Case 1, the actual commutation voltages are experiencing similar dynamics by comparing Fig. 16(b) and Fig. 16(c) with Fig. 15(b) and Fig. 15(c). As discussed in Case 1, this is understandable because the increase of voltage rating of controllable capacitor has limited impact on the actual commutation voltages as shown in Fig. 16(d). Similar to the results comparison from Case 1, the sequence current injections shown in Fig. 16(i) are similar to those shown in Fig. 15(h) with the proposed method.

V. CONCLUSION

This paper has theoretically shown that single-phase fault has different levels of adverse impact on commutations of two 6-pulse bridges in a 12-pulse HVDC scheme. It has shown that the phase shifts of un-faulted phases can be significant (which have long been neglected in previous studies), thereby having large impact on the commutation performance. Based on the theoretical analysis, for AC Filterless Flexible LCC HVDC, this paper has demonstrated that the required voltage rating of controllable capacitors in Y-Δ bridge can be 25% lower than that in Y-Y bridge without compromising the commutation performance. It leads to direct reductions of equipment cost and losses from controllable capacitors. From

a wider perspective, this research lays a theoretical foundation and opens up exciting opportunities in developing new and more efficient methods in addressing the challenge of CF in LCC HVDC systems.

REFERENCES

[1] Y. Xue, X.-P. Zhang, and C. Yang, "AC filterless flexible LCC HVDC with reduced voltage rating of controllable capacitors," *IEEE Trans. Power Syst.*, vol. 33, no. 5, pp. 5507–5518, Sep. 2018.
[2] Y. Xue, X.-P. Zhang, and C. Yang, "Elimination of commutation failures of LCC HVDC system with controllable capacitors," *IEEE Trans. Power Syst.*, vol. 31, no. 4, pp. 3289–3299, Jul. 2016.
[3] P. Kundur, *Power System Stability and Control*. New York, NY, USA: McGraw-Hill, 1994.
[4] *Commutation Failures—Causes and Consequences*, Technical Brochure 103, CIGRE, Working, Group, and 14.05, Paris, France, 1995.
[5] C.-K. Kim, V. K. Sood, G.-S. Jang, S.-J. Lim, K. Electric, and S.-J. Lee, *HVDC Transmission: Power Conversion Applications in Power Systems*. Hoboken, NJ, USA: Wiley, 2009.
[6] C. V. Thio, J. B. Davies, and K. L. Kent, "Commutation failures in HVDC transmission systems," *IEEE Trans. Power Del.*, vol. 11, no. 2, pp. 946–957, Apr. 1996.
[7] W. Yao, C. Liu, J. Fang, X. Ai, J. Wen, and S. Cheng, "Probabilistic analysis of commutation failure in LCC-HVDC system considering the CFPREV and the initial fault voltage angle," *IEEE Trans. Power Del.*, vol. 35, no. 2, pp. 715–724, Apr. 2020.
[8] S. Mirsaeidi and X. Dong, "An enhanced strategy to inhibit commutation failure in line-commutated converters," *IEEE Trans. Ind. Electron.*, vol. 67, no. 1, pp. 340–349, Jan. 2020.
[9] Q. Wang, C. Zhang, X. Wu, and Y. Tang, "Commutation failure prediction method considering commutation voltage distortion and DC current variation," *IEEE Access*, vol. 7, pp. 96531–96539, 2019.
[10] Z. Wei, W. Fang, and J. Liu, "Variable extinction angle control strategy based on virtual resistance to mitigate commutation failures in HVDC system," *IEEE Access*, vol. 8, pp. 93692–93704, 2020.
[11] Y. Lei, T. Li, Q. Tang, Y. Wang, C. Yuan, X. Yang, and Y. Liu, "Comparison of UPFC, SVC and STATCOM in improving commutation failure immunity of LCC-HVDC systems," *IEEE Access*, vol. 8, pp. 135298–135307, 2020.
[12] H. Lihua and R. Yacamini, "Calculation of harmonic interference in HVDC systems with unbalance," in *Proc. Int. Conf. AC DC Power Transmiss.*, Sep. 1991, pp. 390–394.
[13] O. Wasynczuk, "Analysis of line-commutated converters during unbalanced operating conditions," *IEEE Trans. Energy Convers.*, vol. 9, no. 2, pp. 420–426, Jun. 1994.
[14] S. E. M. de Oliveira and J. O. R. P. Guimaraes, "Effects of voltage supply unbalance on AC harmonic current components produced by AC/DC converters," *IEEE Trans. Power Del.*, vol. 22, no. 4, pp. 2498–2507, Oct. 2007.
[15] S. Mirsaeidi, X. Dong, D. Tzelepis, D. M. Said, A. Dysko, and C. Booth, "A predictive control strategy for mitigation of commutation failure in LCC-based HVDC systems," *IEEE Trans. Power Electron.*, vol. 34, no. 1, pp. 160–172, Jan. 2019.
[16] M. Daryabak, S. Filizadeh, and A. B. Vandaei, "Dynamic phasor modeling of LCC-HVDC systems: Unbalanced operation and commutation failure," *Can. J. Electr. Comput. Eng.*, vol. 42, no. 2, pp. 121–131, 2019.
[17] L. Zhang and L. Dofnas, "A novel method to mitigate commutation failures in HVDC systems," in *Proc. Int. Conf. Power Syst. Technol.*, Oct. 2002, pp. 51–56.
[18] H.-I. Son and H.-M. Kim, "An algorithm for effective mitigation of commutation failure in high-voltage direct-current systems," *IEEE Trans. Power Del.*, vol. 31, no. 4, pp. 1437–1446, Aug. 2016.
[19] S. Tamai, H. Naitoh, F. Ishiguro, M. Sato, K. Yamaji, and N. Honjo, "Fast and predictive HVDC extinction angle control," *IEEE Trans. Power Syst.*, vol. 12, no. 3, pp. 1268–1275, Aug. 1997.
[20] M. Szechtman, T. Wess, and C. V. Thio, "A benchmark model for HVDC system studies," in *Proc. Int. Conf. AC DC Power Transmiss.*, Sep. 1991, pp. 374–378.
[21] M. H. Bollen, *Understanding Power Quality Problems: Voltage Sags and Interruptions*. Hoboken, NJ, USA: Wiley, 2000.
[22] M. H. J. Bollen, W. Ping, and N. Jenkins, "Analysis and consequences of the phase jump associated with a voltage sag," in *Proc. 12th Power Syst. Comput. Conf.*, Dresden, Germany, Aug. 1996, pp. 316–322.
[23] *D3.1 Technology Assessment From 2030 to 2050*, document e-HIGHWAY2050, 2014.
[24] G. Alstom, *HVDC Connecting to the Future*. Saint-Ouen, France: Alstom Grid publishers, 2010.
[25] A. Gavrilovic, "AC/DC system strength as indicated by short circuit ratios," in *Proc. Int. Conf. AC DC Power Transmiss.*, Sep. 1991, pp. 27–32.
[26] M. A. Pai, *Energy Function Analysis for Power System Stability*. Norwell, MA, USA: Kluwer, Aug. 1989.

CONGHUAN YANG received the B.Eng. degree in electronic and electrical engineering from the Huazhong University of Science and Technology, Wuhan, China, and the University of Birmingham, Birmingham, U.K., in 2013, and the Ph.D. degree in electronic and electrical engineering from the University of Birmingham, in 2018. She is currently a Research Fellow with the University of Birmingham. Her research interests include power system EMTP simulation and HVDC modeling and control.

YING XUE (Member, IEEE) received the B.Eng. degree in electronic and electrical engineering from the Huazhong University of Science and Technology, Wuhan, China, and the University of Birmingham, Birmingham, U.K., in 2012, and the Ph.D. degree in electronic and electrical engineering from the University of Birmingham, in 2016. He is currently a Lecturer with the University of Birmingham. His main research interests include HVDC modeling and control and power system simulation technology. He is the Secretary and a Treasurer of CIGRE UK NGN and the elected Vice-Chair of CIGRE UK NGN for 2021.

XIAO-PING ZHANG (Fellow, IEEE) received the B.Eng., M.Sc., and Ph.D. degrees in electrical engineering from Southeast University, China, in 1988, 1990, and 1993, respectively.

He was an Associate Professor with the University of Warwick, U.K. From 1993 to 1998, he was with the China State Grid EPRI (NARI Group) on EMS/DMS advanced application software research and development. From 1998 to 1999, he was visiting UMIST. From 1999 to 2000, he was an Alexander-von-Humboldt Research Fellow with the University of Dortmund, Germany. He is currently a Professor of electrical power systems with the University of Birmingham, U.K. He is also the Director of the Smart Grid, Birmingham Energy Institute. He has coauthored the first and second edition of the monograph Flexible AC Transmission Systems: Modeling and Control, published by Springer in 2006, and 2012. He has coauthored the book *Restructured Electric Power Systems: Analysis of Electricity Markets with Equilibrium Models*, published by IEEE Press/Wiley, 2010. His research interests include modeling and control of HVDC, FACTS and renewable energy, distributed generation control, energy market operations, and power system planning.

Dr. Zhang has been made a Fellow of IEEE for contributions to modeling and control of high-voltage dc and ac transmission systems. He is an IEEE PES Distinguished Lecturer on HVDC, FACTS and Wave Energy Generation. He is the Chair of the IEEE WG on Test Systems for Economic Analysis. He is an Advisor to the IEEE PES UK & Ireland Chapter. He has been appointed recently to the Expert Advisory Group of UK Government's Offshore Transmission Network Review.